Data in Brief 54 (2024) 110392

Contents lists available at ScienceDirect

Data in Brief

journal homepage: www.elsevier.com/locate/dib

Data Article

Dataset and measurements from a current density sensor during experimental testing of dynamic load cycling for a parallel-serpentine design of a proton exchange membrane fuel cell

Baltasar Toharias[a,*], Christian Suárez[a], Alfredo Iranzo[a,b], María Salva[a], Felipe Rosa[a]

[a] *Energy Engineering Department, School of Engineering, University of Seville, Camino de los Descubrimientos s/n, 41092 Seville, Spain*
[b] *AICIA - Andalusian Association for Research & Industrial Cooperation, Thermal Engineering Group, Camino de los Descubrimientos s/n, 41092 Seville, Spain*

ARTICLE INFO

Article history:
Received 30 January 2024
Revised 1 April 2024
Accepted 3 April 2024
Available online 5 April 2024

Dataset link: PEMFC_Parallel-Serpentine (Original data)

Keywords:
PEMFC
Polarization curve
Dynamic load cycle
Current density mapping

ABSTRACT

A dataset from experimental tests of a proton exchange membrane fuel cell (PEMFC) with an active area of approximately 50 cm^2, parallel-serpentine channels and cross-flow field distribution between anode and cathode is presented. Tests were performed for four different gas inlet and outlet configurations. In particular, tests were performed for the original configuration, hydrogen inlet and outlet reversed, air inlet and outlet reversed, and hoses reversed for both gases. The operating conditions for all gas configurations were: pressure of 0.5 bar, temperature of 65 °C, anode and cathode relative humidity of 60 %, and anode and cathode stoichiometry of 1.3 and 2.5 respectively. The tests performed were the polarization curve (PC) for each gas configuration and the dynamic load cycles (FC-DLC) also for each hose position. A

Abbreviations: CDM, Current Density Mapping; FC-DLC, Fuel Cell-Dynamic Load Cycle; GDL, Gas Diffusion Layer; IV, Intensity-Voltage; JRC, Joint Research Center; MEA, Membrane Electrode Assembly; MPL, Microporous Layer; OCV, Open Circuit Voltage; PC, Polarization Curve; PEMFC, Proton Exchange Membrane Fuel Cell; P&ID, Piping and Instrumentation Diagram; PLC, Programmable Logic Controller; SCADA, Supervisory Control and Data Acquisition.

* Corresponding author.
E-mail address: btoharias@us.es (B. Toharias).

https://doi.org/10.1016/j.dib.2024.110392

current density mapping (CDM) sensor, capable of measuring both the current density distribution and the temperature distribution inside the cell, was inserted into the fuel cell system during all tests. The use of the sensor during the experiments makes it possible to know how these distributions behave and to observe whether or not there is homogeneity in its measurements, thus verifying that the design of the flow channels is adequate and fulfilling its function. The results can be used to investigate and compare other bipolar plates and channel designs, or to compare with results from other test benches and environmental conditions.

Specifications Table

Subject	Energy
Specific subject area	Experimental data from a bipolar plate parallel-serpentine channel PEM fuel cell during polarization curve and dynamic load cycle tests. Using a current density sensor during the tests and varying the gas inlet/outlet configuration.
Data format	Raw (file in .txt and .csv format)
Type of data	Tables Images Data files with current density and temperature measurements Data files for polarization curves and dynamic load cycles
Data collection	The experimental work was performed in a PEM fuel cell test station designed by the National Hydrogen and Fuel Cell Technology Testing Center (CNH2) at the University of Seville. The test station is dedicated to the experimental testing of single PEMFCs and stacks up to 500 W. The control system of the test bench is based on a PLC capable of real time control, allowing it to operate safely and autonomously. Parallel to the PLC, there is a computer with control logging of all generated data, serving as an interface via a graphical SCADA. The fuel cell test has bipolar graphite plates from ElectroChem Inc. with an active area of approximately 50 cm^2. The channel design presents a parallel-serpentine layout at both the anode and cathode, arranged in a cross-flow, i.e., the anode channels are horizontal and the cathode channels are vertical. The current density mapping sensor was supplied by *S*++ Simulation Services and CurrentVIEW software was used to obtain the current density and temperature distribution measurements of the tests. The sensor was installed between the bipolar plate and the current collector of the cathode zone. The polarization curves and dynamic load cycles were performed according to the JRC protocol. In addition, the configuration of the inlets and outlets of the gas hoses was modified.
Data source location	• Institution: University of Seville • City: Seville • Country: Spain
Data accessibility	Repository name: idUS Data identification number: 11,441/153,760 Direct URL to data: https://idus.us.es/handle/11441/153760
Related research article	C. Suárez, B. Toharias, M. Salva, A. Chesalkin, F. Rosa, A. Iranzo, Experimental dynamic load cycling and current density measurements of different inlet/outlet configurations of a parallel-serpentine PEMFC, Energy 283 (2023) 128,455 https://doi.org/10.1016/j.energy.2023.128455

1. Value of the Data

- This dataset containing polarization curves and dynamic load cycle tests for a PEM fuel cell provides a basis for conducting such tests. They show the performance of the cell with the parallel-serpentine bipolar plate and how the fuel cell would perform under operation in a driving cycle. The temperature and current density data measured by the CDM sensor allow an understanding of the internal behavior, and even how the measuring device and software needs to be configured. The data showing the internal temperature and current density distribution within PEMFCs is lacking in the open literature, and the published data is contributing to make this data available for the scientific community, to foster a better understanding of the internal cell processes and behavior, and also providing experimental data for detailed model validation.
- The data generated can be used by researchers and engineers in the field of PEM fuel cell research and development. They are intended to provide deeper knowledge, information and understanding of the different variables involved in PEM fuel cell testing. Advanced modeling of PEMFCs such as Computational Fluid Dynamics modeling can make a thorough use of the data, as this kind of experimental measurements of internal distribution of variables is required for a comprehensive model validation.
- The data obtained from different test benches can be used to compare polarization curves and driving cycles to check that the results obtained are reproducible and that the use of a different test bench or environmental conditions does not affect the results. The data provided by the CDM sensor allows analysis of how temperatures and current densities are distributed across the plate. This makes it possible to optimize the design if there is insufficient homogeneity in the measurements in any area and there are significant irregularities. The operating conditions and gas flow configuration are comprehensively described in this work so that it allows for potential replicability at other laboratories and test benches. Data can be used for research activities related to cell heat management and adapted to perform model validation.

2. Background

The data article adds information to the previously published article. This article includes the dataset used in the full-length article to conduct the research. It clearly defines the published data and how all variables are named, indicating the format in which the test bench and CDM sensor files were exported. In addition, it explains in more detail the components used to perform the test and obtain this dataset, including also how these components have been assembled in the fuel cell system. The experimental test has been described indicating the protocol followed and the use of the CDM sensor and its software in the data acquisition. In short, this data article shows the whole process followed in the development of the research, from the description of the materials used and the assembly of the fuel cell to the obtaining of the test data, complemented by the full-length article that interprets the results.

3. Data Description

3.1. Data file: PEMFC_Parallel-Serpentine.zip

The data presented in this paper are based on the experimental results of a PEM fuel cell with a parallel-serpentine bipolar plate design. Two types of tests have been performed, firstly polarization curve tests and secondly dynamic load cycling tests. The results of these tests are discussed and interpreted in the full paper "C. Suárez, B. Toharias, M. Salva, A. Chesalkin, F. Rosa, A. Iranzo, Experimental dynamic load cycling and current density measurements of different inlet/outlet configurations of a parallel-serpentine PEMFC" [1]. The experimental tests were performed according to the JRC protocol [2]. The current density distribution and temperature distribution datasets obtained in this series of experimental tests are significant in the field of PEMFCs, as demonstrated by other researchers in their recent studies. Zhou et al. [3] provide a basis for developing an optimal thermal management system through local optimization of channels and achieving more uniform temperature and current density distributions. These distributions result in improved fuel cell performance and extended lifetime. Gao et al. [4] propose a water flooding diagnosis method based on current density scanning, which can quantify the severity of flooding and determine the location of flooding by measuring the changes in current density distribution. Ding et al. [5] characterize possible holes in the MEA due to degradation during operation or fabrication by current density distribution and temperature.

The dataset provided is organized following the schematic in Fig. 1. The results are differentiated according to the four reagent inlet and outlet configurations. Normal flow (*Normal_Flow, NF*) was referred to when the reagent inlet and outlet hoses were connected in accordance with the original ElectroChem fuel cell design. When the hydrogen flow connection was reversed, it was called inverse hydrogen flow (*Inverse_Hydrogen_Flow, IHF*). In this case, the hydrogen inlet and outlet were reversed while the air flow remained in its original configuration. On the contrary, if the air flow direction was reversed but the hydrogen flow remained in its original configuration, it was named as inverse air flow (*Inverse_Air_Flow, IAF*). And the last case consisted of inverting both gas flows, exchanging the inlets for the outlets in the air and hydrogen hoses, and it was named as inverse flow (*Inverse_Flow, IF*). Fig. 2 shows how these four gas configurations are connected in the cell through a schematic and a picture of the real fuel cell. Another classification of the data provided was the type of test performed, distinguishing between dynamic load cycles (*FC-DLC*) and polarization curves (*PC*).

The following nomenclature was used to name the data folders: *AA_BB_CC_***P***DD_***T***EE_***a***FF***RH***GG_***c***HH***RH***II***air** where *AA* indicates the configuration of the gas hoses, *BB* is the type of test performed, *CC* is the date on which experiment was performed, *DD* is the operating pressure in bar with a decimal, *EE* is the operating temperature in Celsius, *FF* is the anode stoichiometry with a decimal, *GG* is the anode relative humidity in%, *HH* is the cathode stoichiometry with a decimal, and II is the cathode relative humidity in%. The word *air* is indicated at the end to show that the experiment was carried out feeding air instead of pure oxygen in the cathode. For example, *NF_FC-DLC_20220209_P05_T65_a13RH60_c25RH60air, NF* indicates that a normal gas flow configuration was used, *FC-DLC* indicates that it is a dynamic load cycling test, *20220209* indicates the date (year 2022, month 02 and day 09) and *P05_T65_a13RH60_c25RH60air* indicates the test operating conditions: $P = 0.5$ bar, $T = 65$ °C, λ_a=1.3, RH_a=60 %, λ_c=2.5, RH_c=60%.

Inside each folder are three data files: two files with the CDM sensor data in .dat format, and one file with the data recorded on the test bench in .csv format. The first two are named **CDM**_*JJ_CC_***P***DD_***T***EE_***a***FF***RH***GG_***c***HH***RH***II***air**, where *JJ* is marked as *C* if the data are the current density measurements obtained with the sensor in A/segment, while it is marked as *T* when the data are the temperature measurements in Celsius. The test bench data file is named *BB_CC_***P***DD_***T***EE_***a***FF***RH***GG_***c***HH***RH***II***air**.

On the one hand, the files with the data obtained by the CDM sensor are organized in the form of data matrices. For the results of current distribution, the data matrix is 18 × 18 (e.g., *CDM_C_20220209_P05_T65_a13RH60_c25RH60air.dat*), while the matrix with the results of temperature distribution inside the fuel cell is 9 × 9 (e.g., *CDM_T_20220209_P05_T65_a13RH60_c25RH60air.dat*). The origin of the sensor is located in the lower right corner of the gold plate or measuring plate, as can be seen in Fig. 3.

Once the origin is defined and located, the current and temperature distribution variables can be named. The temperature distribution was named $T_{a,b}$, where *a* is the row of the matrix and *b* is the column. Fig. 4 shows how all the variables are located in a schematic and on the real measurement plate of the CDM sensor. In addition, Fig. 5 shows an example of the data obtained in a test, specifically for the polarization curve test, showing first the date the test was performed, then a reference number from the date and finally the temperature matrix.

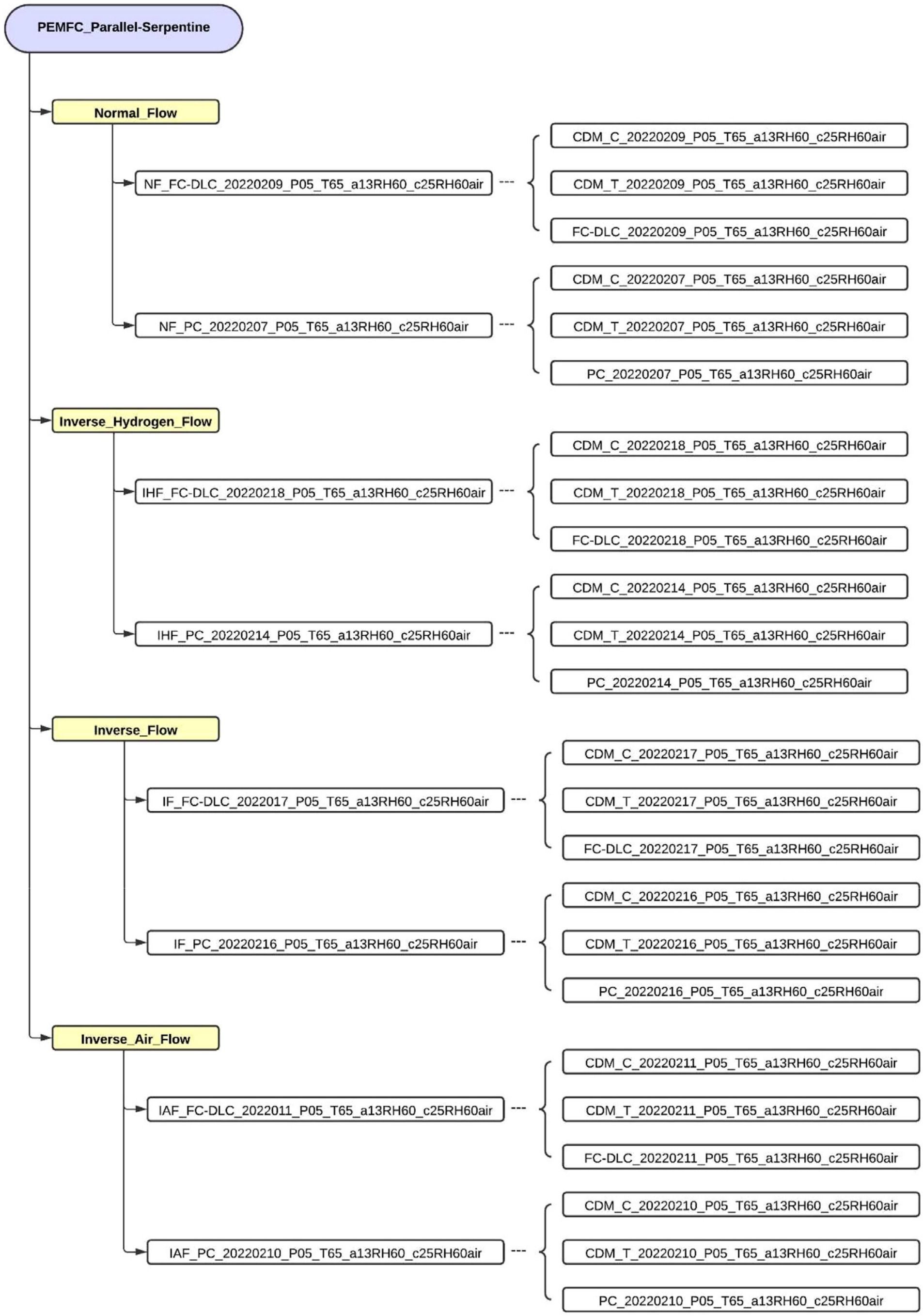

Fig. 1. Diagram of dataset files.

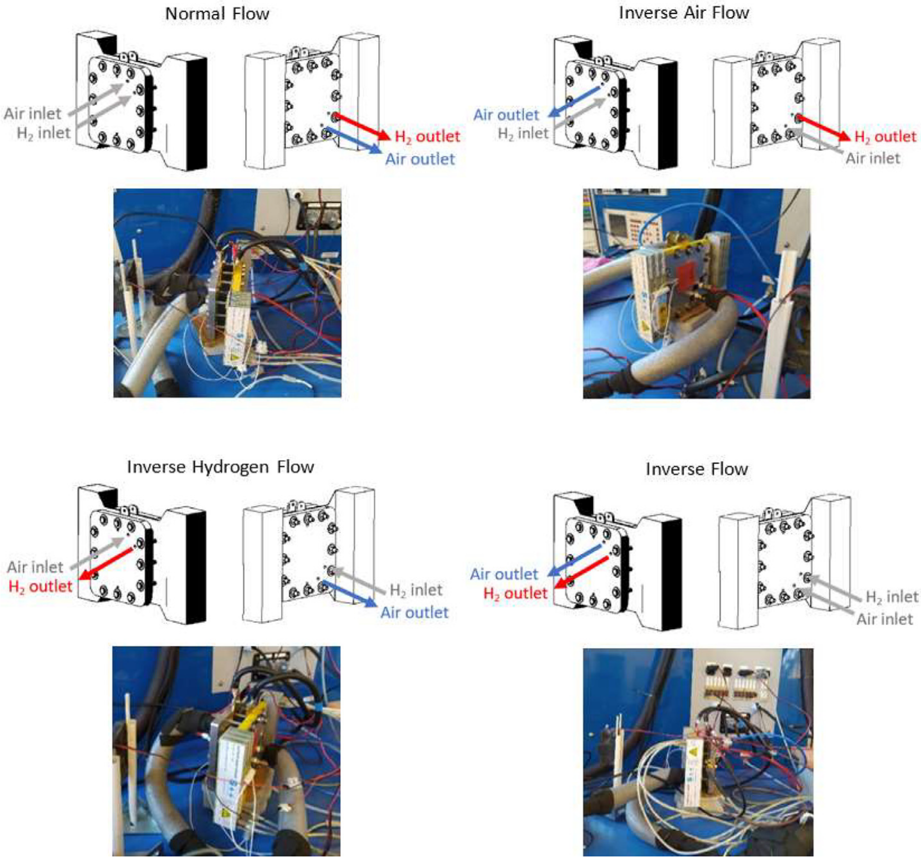

Fig. 2. Diagram of the four gas inlet/outlet configurations.

The current distribution data is called $C_{a,b}$ and is organized as shown in Fig. 6. Fig. 7 shows an example of the data exported by the CDM sensor in the test performed to obtain the polarization curve, showing first the date the test was performed, then a reference number from the date and finally the current density matrix. The data obtained for the current distribution case were negative due to the polarity reversal of the CDM sensor, but this did not affect the values and therefore the development of the tests. To correct this mismatch, the sign of these current density values was inverted in the post-processing of the data.

On the other hand, the files exported by the test bench with the results of the experiments to obtain the polarization curve (e.g., *PC_20220207_P05_T65_a13RH60_c25RH60air.csv*) or the dynamic load cycles (e.g., *FC-DLC_20220209_P05_T65_a13RH60_c25RH60air.csv*) contain information such as the temperature or the pressure of the cell in each second of the test, or the intensity generated by the fuel cell. In Table 1 it is possible to see each of the variables that appear in these files, with a brief description of what each data is and the unit of measurement, if applicable, to help the future user of this dataset.

Finally, Fig. 8 shows the first data of the test programmed in the bench to obtain the polarization curve.

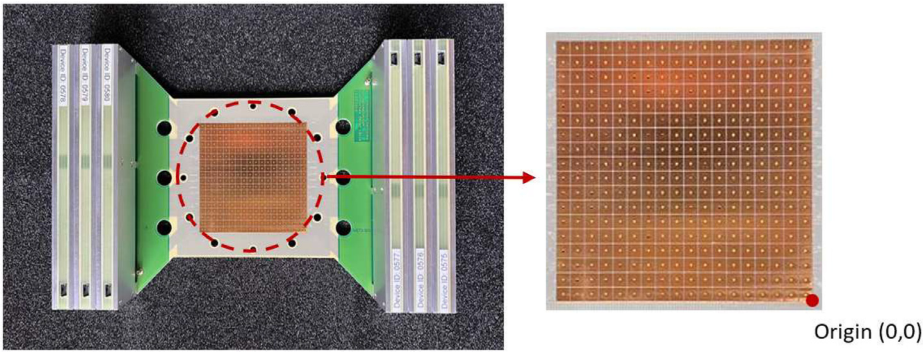

Fig. 3. Origin of CDM sensor coordinates.

$\mathbf{T_{1,1}}$	$T_{1,2}$	$T_{1,3}$	$T_{1,4}$	$T_{1,5}$	$T_{1,6}$	$T_{1,7}$	$T_{1,8}$	$T_{1,9}$
$T_{2,1}$	$\mathbf{T_{2,2}}$	$T_{2,3}$	$T_{2,4}$	$T_{2,5}$	$T_{2,6}$	$T_{2,7}$	$T_{2,8}$	$T_{2,9}$
$T_{3,1}$	$T_{3,2}$	$\mathbf{T_{3,3}}$	$T_{3,4}$	$T_{3,5}$	$T_{3,6}$	$T_{3,7}$	$T_{3,8}$	$T_{3,9}$
$T_{4,1}$	$T_{4,2}$	$T_{4,3}$	$\mathbf{T_{4,4}}$	$T_{4,5}$	$T_{4,6}$	$T_{4,7}$	$T_{4,8}$	$T_{4,9}$
$T_{5,1}$	$T_{5,2}$	$T_{5,3}$	$T_{5,4}$	$\mathbf{T_{5,5}}$	$T_{5,6}$	$T_{5,7}$	$T_{5,8}$	$T_{5,9}$
$T_{6,1}$	$T_{6,2}$	$T_{6,3}$	$T_{6,4}$	$T_{6,5}$	$\mathbf{T_{6,6}}$	$T_{6,7}$	$T_{6,8}$	$T_{6,9}$
$T_{7,1}$	$T_{7,2}$	$T_{7,3}$	$T_{7,4}$	$T_{7,5}$	$T_{7,6}$	$\mathbf{T_{7,7}}$	$T_{7,8}$	$T_{7,9}$
$T_{8,1}$	$T_{8,2}$	$T_{8,3}$	$T_{8,4}$	$T_{8,5}$	$T_{8,6}$	$T_{8,7}$	$\mathbf{T_{8,8}}$	$T_{8,9}$
$T_{9,1}$	$T_{9,2}$	$T_{9,3}$	$T_{9,4}$	$T_{9,5}$	$T_{9,6}$	$T_{9,7}$	$T_{9,8}$	$\mathbf{T_{9,9}}$

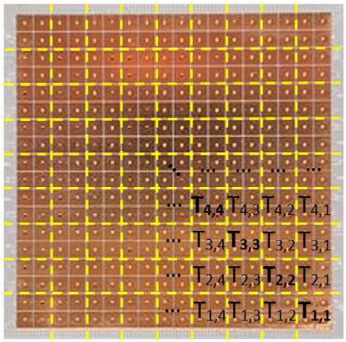

Fig. 4. CDM sensor variables for temperature measurements (9 × 9).

07/02/22 20:40:20.141
3727107620.142

temperature

67.9246	67.9807	68.0675	68.1115	67.9950	68.0343	67.6490	67.5919	67.4679
67.8279	68.0492	68.0021	68.3172	67.9259	68.1777	67.6515	67.5711	67.3712
67.9370	68.0494	68.1538	68.2643	68.1112	68.2061	67.6938	67.6379	67.5019
67.9451	67.9668	68.1168	68.2273	68.1484	68.1155	67.7943	67.5600	67.4382
67.7997	68.0456	68.1831	68.3643	68.2131	68.2312	67.7851	67.6494	67.3980
67.7618	67.9318	68.1512	68.3057	68.1394	68.0721	67.8455	67.5480	67.3605
67.6705	67.8724	67.9018	68.2478	67.9862	67.9262	67.6792	67.4564	67.3813
67.5695	67.7394	67.7381	68.1348	67.6631	67.9431	67.4206	67.4203	67.2874
67.6032	67.6635	67.5659	67.9720	67.5951	67.5949	67.4443	67.2743	67.2623

Fig. 5. Example of temperature distribution in the polarization curve test.

$\mathbf{C_{1,1}}$	$C_{1,2}$	$C_{1,3}$	$C_{1,4}$	$C_{1,5}$	$C_{1,6}$	$C_{1,7}$	$C_{1,8}$	$C_{1,9}$	$C_{1,10}$	$C_{1,11}$	$C_{1,12}$	$C_{1,13}$	$C_{1,14}$	$C_{1,15}$	$C_{1,16}$	$C_{1,17}$	$C_{1,18}$
$C_{2,1}$	$\mathbf{C_{2,2}}$	$C_{2,3}$	$C_{2,4}$	$C_{2,5}$	$C_{2,6}$	$C_{2,7}$	$C_{2,8}$	$C_{2,9}$	$C_{2,10}$	$C_{2,11}$	$C_{2,12}$	$C_{2,13}$	$C_{2,14}$	$C_{2,15}$	$C_{2,16}$	$C_{2,17}$	$C_{2,18}$
$C_{3,1}$	$C_{3,2}$	$\mathbf{C_{3,3}}$	$C_{3,4}$	$C_{3,5}$	$C_{3,6}$	$C_{3,7}$	$C_{3,8}$	$C_{3,9}$	$C_{3,10}$	$C_{3,11}$	$C_{3,12}$	$C_{3,13}$	$C_{3,14}$	$C_{3,15}$	$C_{3,16}$	$C_{3,17}$	$C_{3,18}$
$C_{4,1}$	$C_{4,2}$	$C_{4,3}$	$\mathbf{C_{4,4}}$	$C_{4,5}$	$C_{4,6}$	$C_{4,7}$	$C_{4,8}$	$C_{4,9}$	$C_{4,10}$	$C_{4,11}$	$C_{4,12}$	$C_{4,13}$	$C_{4,14}$	$C_{4,15}$	$C_{4,16}$	$C_{4,17}$	$C_{4,18}$
$C_{5,1}$	$C_{5,2}$	$C_{5,3}$	$C_{5,4}$	$\mathbf{C_{5,5}}$	$C_{5,6}$	$C_{5,7}$	$C_{5,8}$	$C_{5,9}$	$C_{5,10}$	$C_{5,11}$	$C_{5,12}$	$C_{5,13}$	$C_{5,14}$	$C_{5,15}$	$C_{5,16}$	$C_{5,17}$	$C_{5,18}$
$C_{6,1}$	$C_{6,2}$	$C_{6,3}$	$C_{6,4}$	$C_{6,5}$	$\mathbf{C_{6,6}}$	$C_{6,7}$	$C_{6,8}$	$C_{6,9}$	$C_{6,10}$	$C_{6,11}$	$C_{6,12}$	$C_{6,13}$	$C_{6,14}$	$C_{6,15}$	$C_{6,16}$	$C_{6,17}$	$C_{6,18}$
$C_{7,1}$	$C_{7,2}$	$C_{7,3}$	$C_{7,4}$	$C_{7,5}$	$C_{7,6}$	$\mathbf{C_{7,7}}$	$C_{7,8}$	$C_{7,9}$	$C_{7,10}$	$C_{7,11}$	$C_{7,12}$	$C_{7,13}$	$C_{7,14}$	$C_{7,15}$	$C_{7,16}$	$C_{7,17}$	$C_{7,18}$
$C_{8,1}$	$C_{8,2}$	$C_{8,3}$	$C_{8,4}$	$C_{8,5}$	$C_{8,6}$	$C_{8,7}$	$\mathbf{C_{8,8}}$	$C_{8,9}$	$C_{8,10}$	$C_{8,11}$	$C_{8,12}$	$C_{8,13}$	$C_{8,14}$	$C_{8,15}$	$C_{8,16}$	$C_{8,17}$	$C_{8,18}$
$C_{9,1}$	$C_{9,2}$	$C_{9,3}$	$C_{9,4}$	$C_{9,5}$	$C_{9,6}$	$C_{9,7}$	$C_{9,8}$	$\mathbf{C_{9,9}}$	$C_{9,10}$	$C_{9,11}$	$C_{9,12}$	$C_{9,13}$	$C_{9,14}$	$C_{9,15}$	$C_{9,16}$	$C_{9,17}$	$C_{9,18}$
$C_{10,1}$	$C_{10,2}$	$C_{10,3}$	$C_{10,4}$	$C_{10,5}$	$C_{10,6}$	$C_{10,7}$	$C_{10,8}$	$C_{10,9}$	$\mathbf{C_{10,10}}$	$C_{10,11}$	$C_{10,12}$	$C_{10,13}$	$C_{10,14}$	$C_{10,15}$	$C_{10,16}$	$C_{10,17}$	$C_{10,18}$
$C_{11,1}$	$C_{11,2}$	$C_{11,3}$	$C_{11,4}$	$C_{11,5}$	$C_{11,6}$	$C_{11,7}$	$C_{11,8}$	$C_{11,9}$	$C_{11,10}$	$\mathbf{C_{11,11}}$	$C_{11,12}$	$C_{11,13}$	$C_{11,14}$	$C_{11,15}$	$C_{11,16}$	$C_{11,17}$	$C_{11,18}$
$C_{12,1}$	$C_{12,2}$	$C_{12,3}$	$C_{12,4}$	$C_{12,5}$	$C_{12,6}$	$C_{12,7}$	$C_{12,8}$	$C_{12,9}$	$C_{12,10}$	$C_{12,11}$	$\mathbf{C_{12,12}}$	$C_{12,13}$	$C_{12,14}$	$C_{12,15}$	$C_{12,16}$	$C_{12,17}$	$C_{12,18}$
$C_{13,1}$	$C_{13,2}$	$C_{13,3}$	$C_{13,4}$	$C_{13,5}$	$C_{13,6}$	$C_{13,7}$	$C_{13,8}$	$C_{13,9}$	$C_{13,10}$	$C_{13,11}$	$C_{13,12}$	$\mathbf{C_{13,13}}$	$C_{13,14}$	$C_{13,15}$	$C_{13,16}$	$C_{13,17}$	$C_{13,18}$
$C_{14,1}$	$C_{14,2}$	$C_{14,3}$	$C_{14,4}$	$C_{14,5}$	$C_{14,6}$	$C_{14,7}$	$C_{14,8}$	$C_{14,9}$	$C_{14,10}$	$C_{14,11}$	$C_{14,12}$	$C_{14,13}$	$\mathbf{C_{14,14}}$	$C_{14,15}$	$C_{14,16}$	$C_{14,17}$	$C_{14,18}$
$C_{15,1}$	$C_{15,2}$	$C_{15,3}$	$C_{15,4}$	$C_{15,5}$	$C_{15,6}$	$C_{15,7}$	$C_{15,8}$	$C_{15,9}$	$C_{15,10}$	$C_{15,11}$	$C_{15,12}$	$C_{15,13}$	$C_{15,14}$	$\mathbf{C_{15,15}}$	$C_{15,16}$	$C_{15,17}$	$C_{15,18}$
$C_{16,1}$	$C_{16,2}$	$C_{16,3}$	$C_{16,4}$	$C_{16,5}$	$C_{16,6}$	$C_{16,7}$	$C_{16,8}$	$C_{16,9}$	$C_{16,10}$	$C_{16,11}$	$C_{16,12}$	$C_{16,13}$	$C_{16,14}$	$C_{16,15}$	$\mathbf{C_{16,16}}$	$C_{16,17}$	$C_{16,18}$
$C_{17,1}$	$C_{17,2}$	$C_{17,3}$	$C_{17,4}$	$C_{17,5}$	$C_{17,6}$	$C_{17,7}$	$C_{17,8}$	$C_{17,9}$	$C_{17,10}$	$C_{17,11}$	$C_{17,12}$	$C_{17,13}$	$C_{17,14}$	$C_{17,15}$	$C_{17,16}$	$\mathbf{C_{17,17}}$	$C_{17,18}$
$C_{18,1}$	$C_{18,2}$	$C_{18,3}$	$C_{18,4}$	$C_{18,5}$	$C_{18,6}$	$C_{18,7}$	$C_{18,8}$	$C_{18,9}$	$C_{18,10}$	$C_{18,11}$	$C_{18,12}$	$C_{18,13}$	$C_{18,14}$	$C_{18,15}$	$C_{18,16}$	$C_{18,17}$	$\mathbf{C_{18,18}}$

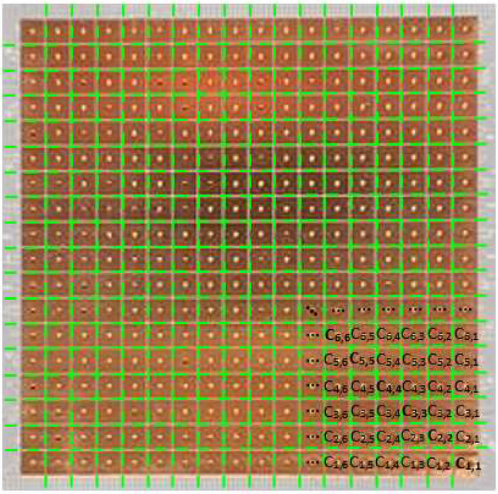

Fig. 6. CDM sensor variables for current density measurements (18 × 18).

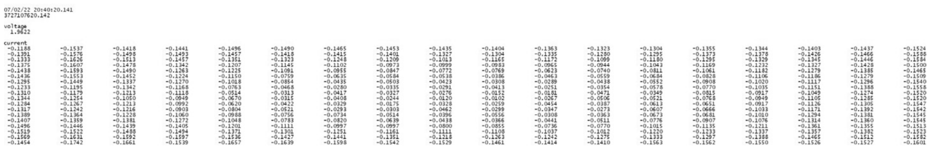

Fig. 7. Example of current density distribution in the polarization curve test.

Table 1
Description of data exported from the test bench.

Variable	Description	Unit
Fecha	Date when the test data was started to be recorded.	–
Hora	Time when the test data was started to be recorded.	–
PT001	Pressure measured by the hydrogen inlet flow.	bar_g
PT002	Pressure measured by the air inlet flow.	bar_g
PT003	Pressure measured by nitrogen inlet flow.	bar_g
PT004	Pressure measured by deionized water in the anode zone humidifier tank.	bar_g
PT005	Pressure measured by the deionized water in the cathodic zone humidifier tank.	bar_g
PT006	Pressure measured by the hydrogen flow at the outlet of the fuel cell.	bar_g
PT007	Pressure measured by the air flow at the outlet of the fuel cell.	bar_g
BP001	Pressure measured by the back pressure regulator on the anode side.	bar_g
BP002	Pressure measured by the back pressure regulator on the cathodic side.	bar_g
FT001	Flow rate measured by the mass flow meter controlling the hydrogen flow in the low range (0.08–2 NL/min).	NL/min
FT002	Flow rate measured by the mass flow meter controlling the hydrogen flow in the high ranges (0.4–14 NL/min).	NL/min
FT003	Flow rate measured by the mass flow meter controlling the air flow in the low range (0.05–1NL/min).	NL/min
FT004	Flow rate measured by the mass flow meter controlling the air flow in the high range (0.95–47.5 NL/min).	NL/min
FT005	Flow rate measured by thermostatic bath.	NL/min
HT001	Relative humidity of the hydrogen inlet flow.	%
HT002	Relative humidity of the air inlet flow.	%
V001	Voltage measured in cell 1.	V
V002	Voltage measured in cell 2.	V
V003	Voltage measured in cell 3.	V
V004	Voltage measured in cell 4.	V
V005	Voltage measured in cell 5.	V
V006	Voltage measured in cell 6.	V
V007	Voltage measured in cell 7.	V
TT001	Temperature of the humidifier water in the anode zone.	°C
TT002	Temperature measured at the outlet of the hydrogen flow humidifier.	°C
TT003	Temperature of the hydrogen flow at the fuel cell inlet.	°C
TT004	Temperature of the hydrogen flow at the fuel cell outlet.	°C
TT005	Temperature of the humidifier water in the cathodic zone.	°C
TT006	Temperature measured at the outlet of the air flow humidifier.	°C
TT007	Temperature of the air flow at the fuel cell inlet.	°C
TT008	Temperature of the air flow at the fuel cell outlet.	°C
TT009	Temperature of the cooling water at the fuel cell inlet.	°C
TT010	Temperature of the cooling water at the fuel cell outlet.	°C
T013	Temperature of the heated hose of the anode zone.	°C
T014	Temperature of the heated hose of the cathodic zone.	°C
INTENSIDAD	Intensity measured in the fuel cell.	A

FECHA	HORA	PT001	PT002	PT003	PT004	PT005	PT006	PT007	BP001	BP002	FT001	FT002
07/02/2022	20:40:44	3.489	3.799	4.297	0.488	0.475	0.501	0.493	0.486	0.322	0.317	0.01
07/02/2022	20:40:45	3.49	3.797	4.297	0.488	0.475	0.501	0.493	0.485	0.321	0.316	0.006
07/02/2022	20:40:46	3.488	3.8	4.296	0.488	0.475	0.501	0.492	0.484	0.324	0.319	0.006
07/02/2022	20:40:47	3.49	3.799	4.296	0.488	0.474	0.501	0.493	0.484	0.322	0.318	0.006
07/02/2022	20:40:48	3.489	3.801	4.297	0.488	0.474	0.501	0.493	0.483	0.322	0.318	0.008
07/02/2022	20:40:49	3.49	3.798	4.297	0.488	0.474	0.501	0.492	0.484	0.322	0.318	0.005
07/02/2022	20:40:50	3.491	3.798	4.297	0.488	0.474	0.501	0.491	0.485	0.322	0.319	0.004
07/02/2022	20:40:51	3.49	3.798	4.296	0.488	0.474	0.501	0.493	0.485	0.321	0.317	0.008
07/02/2022	20:40:52	3.49	3.797	4.296	0.488	0.474	0.501	0.492	0.487	0.322	0.319	0.004
...	...	...	...	...	...	...	...	...	...	...	...	...

FT003	FT004	FT005	HT001	HT002	V001	V002	V003	V004	V005	V006	V007	TT001
0	1.451	0	64.922	0	0.494	-0.165	0	0	0	0.001	0.001	54.1
0	1.419	0	65.208	0	0.495	-0.165	0	0	0	0.001	0.001	54.1
0	1.532	0	65.483	0	0.495	-0.165	0	0	0	0.001	0.001	54.1
0	1.486	0	65.746	0	0.495	-0.165	0	0	0	0.001	0.001	54.1
0	1.506	0	66	0	0.495	-0.165	0	0	0	0.001	0.001	54.1
0	1.478	0	66.244	0	0.495	-0.165	0	0	0	0.001	0.001	54.1
0	1.497	0	66.48	0	0.495	-0.165	0	0	0	0.001	0.001	54.1
0	1.461	0	66.708	0	0.495	-0.165	0	0	0	0.001	0.001	54.1
0	1.508	0	66.93	0	0.495	-0.165	0	0	0	0.001	0.001	54.1
...	...	...	...	...	...	...	...	...	...	...	...	...

TT002	TT003	TT004	TT005	TT006	TT007	TT008	TT009	TT010	TT013	TT014	INTENSIDAD
100.8	65.1	19.8	54	90	65.1	26.8	0	18.6	127.1	114.4	34.91
100.9	65.1	19.7	54	89.9	65.1	26.8	0	18.6	127.1	114.4	34.91
101.1	65.1	19.8	54.1	89.8	65.1	26.8	0	18.6	127.1	114.3	34.91
101.3	65.1	19.8	54	89.8	65.1	26.8	0	18.6	127.1	114.2	34.91
101.5	65.1	19.8	54	89.6	65.1	26.7	0	18.6	127	114.1	34.91
101.6	65.1	19.7	54	89.6	65.1	26.7	0	18.6	127	114.1	34.91
101.8	65.1	19.8	54	89.4	65.1	26.7	0	18.6	127	114.1	34.91
102	65.1	19.7	54	89.4	65.1	26.7	0	18.6	127	113.9	34.91
102.2	65.1	19.8	54	89.3	65.1	26.7	0	18.6	127	113.9	34.91
...	...	...	...	...	...	...	...	...	...	...	...

Fig. 8. Example of test bench data during polarization curve test.

4. Experimental Design, Materials and Methods

The experimental tests were performed in the test bench, which consists of a main structure and several individual compartments to separate and accommodate different working areas. The test bench (Fig. 9) is equipped with a balance of plant to condition all the fuel cell inlet and outlet flows, a thermostatic bath to control the water flow and temperature if water cooling is used, a deionized water production system, a programmable electronic load, or a fume hood. The test station allows the operation of PEMFCs, both single cells and stacks up to 500 W. The control system of the test bench is based on a PLC with the ability to perform real-time controls. This system manages the balance of the plant by controlling all the variables, which through alarms allows the autonomous and safe operation of the plant. Parallel to the PLC, there is a computer in charge of the communication and monitoring operations, serving as a graphical interface with the user through a graphical SCADA.

In the interface, as shown on the left in Fig. 10, there is a section where the operating conditions to be tested can be introduced. It is divided into an anode zone, a cathode zone and a zone called *STACK*. In the anode and cathode zones, the humidity, temperature, pressure or stoichiometry of these lines are controlled, while in the *STACK*, the values of the pressure and temperature of the fuel cell are introduced. On the right side of Fig. 10 is the P&ID showing all the piping and instrumentation of the test bench. This diagram allows the user to visualize in real time the status of the resistors, solenoid valves, etc., or the monitoring of all the sensors and transmitters located in the test bench.

The fuel cell was mounted on a workbench available on the test bench, with a front panel for reaction gas inlets and outlets. In addition, the electronic load, the power supply, and a frequency response analyzer were installed. The tests were performed on a PEM fuel cell, whose distribution and components are described in the schematic in Fig. 11.

1. Screws, nuts and washers.
2. End plates: made of aluminum.
3. Gaskets.
4. Current collectors: gold-plated current collector with a thickness of 2 mm.

Fig. 9. PEM fuel cell test bench.

5. Toray GDLs: the gas diffusion layer between the collector and the anode zone bipolar plate, the collector and the CDM sensor, and the CDM sensor and the cathode bipolar plate was Toray Carbon Paper TP-090-T5 (from Quintech®), with a thickness of 0.28 mm and 5% Teflon treatment.
6. Bipolar plates: made of graphite (from ElectroChem Inc.), with a parallel-serpentine channel design. The gas channels of the anode bipolar plate are arranged vertically, while the channels of the cathode bipolar plate are arranged horizontally, so that it was performed with cross-flow. The parallel-serpentine design consists of 5 channel blocks, which are linked through a 1.5 mm wide and 1.7 mm deep manifold. The dimension of each channel is 0.71 mm wide and 1.1 mm deep, while the ribs are 0.86 mm wide. The active area of the fuel cell is approximately 50 cm^2, specifically 69.8 mm wide and 69.9 mm high, for a total active area of 48.79 cm^2. The plan of the cathode bipolar plate is shown in Fig. 12.
7. MEA: Gore A510.1 / M775.15 / C586.4 (from GORE® PRIMEA®) was selected as the membrane electrode assembly. The MEA has a platinum loading of 0.1 mg/cm^2 on the anode side and 0.4 mg/cm^2 on the cathode side, and it has a thickness of 0.15 mm.
8. Freudenberg GDLs: the gas diffusion layer between the anode bipolar plate and the MEA, and between the cathode bipolar plate and the MEA, was Freudenberg H23C6 (from Quintech®), with a thickness of 0.25 mm and with a hydrophobic treatment or MPL. This MPL helps to minimize the contact resistance between the GDL itself and the catalytic layer of the MEA, and it helps to improve water management by facilitating its transport.
9. CDM sensor: the current density mapping sensor was provided by *S*++ Simulation Services [6]. This sensor (Fig. 13) was placed between the current collector and the bipolar plate of the cathodic zone to measure both current and temperature distribution. It con-

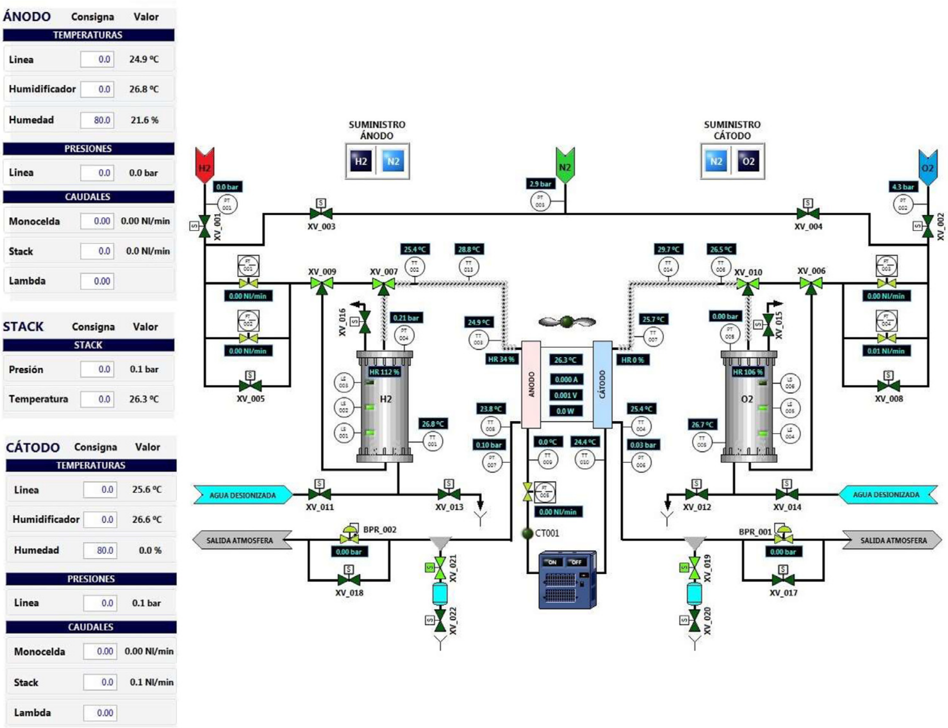

Fig. 10. Graphical test bench interface.

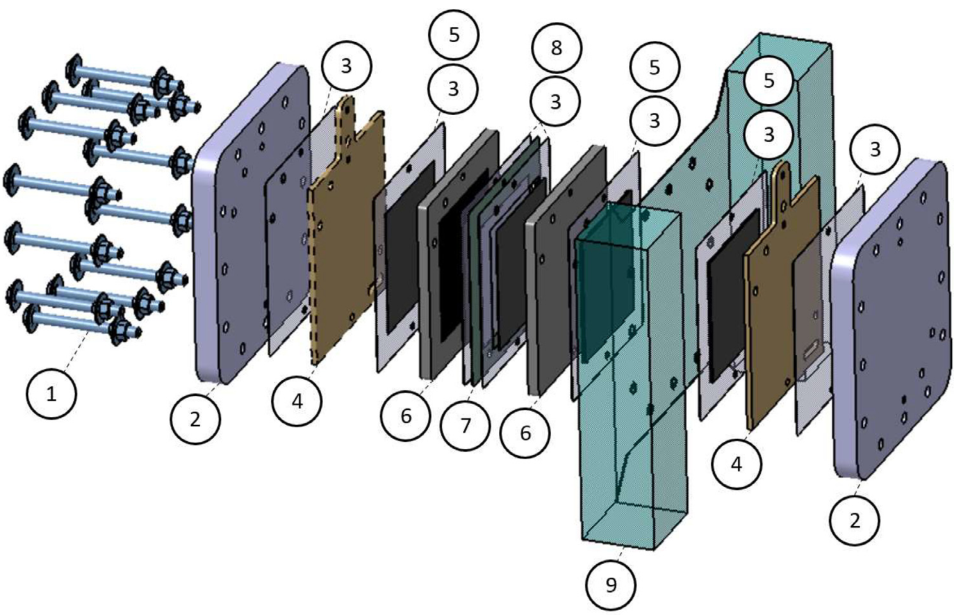

Fig. 11. Schematic arrangement of components used in the fuel cell.

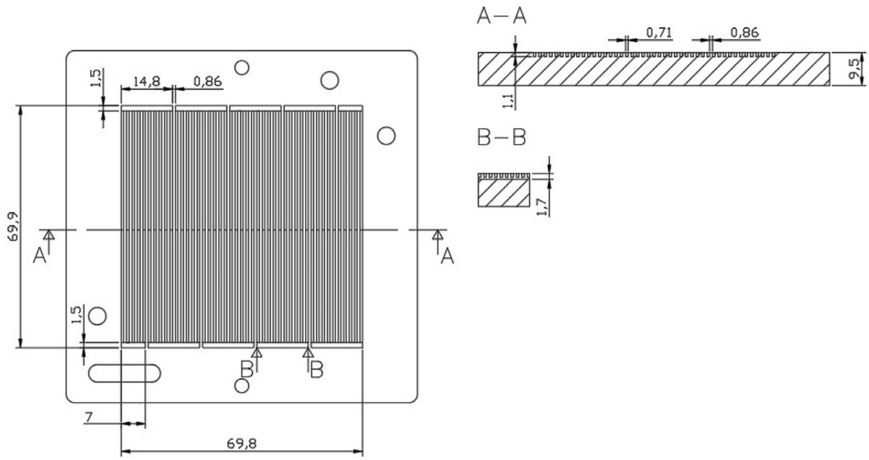

Fig. 12. Cathode bipolar plate drawing with parallel-serpentine design (from ElectroChem Inc.).

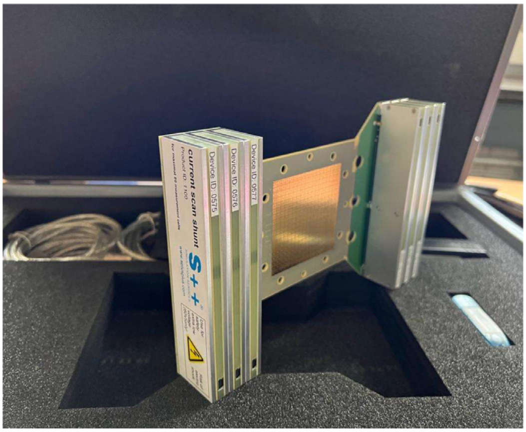

Fig. 13. Current density mapping sensor (CDM).

Table 2
Experimental test operating conditions.

Parameter	Value
Cell temperature	65 °C
Cell pressure	0.5 bar
Relative humidity of anode	60 %
Relative humidity of cathode	60 %
Anode stoichiometric factor	1.3
Cathode stoichiometric factor	2.5

sists of a 0.7 mm thick electronic device, whose measurement plate is gold plated and it has an active area of 50 cm^2.

Once all the components of the fuel cell were assembled and connected to the test bench, the experimental tests began. For the experimental tests of the fuel cell in the four proposed gas configurations, the same operating conditions were maintained as indicated in Table 2.

Table 3
Polarization curve set points.

Set point no.	Current density (A/cm^2)	Time (s)
1	X	3600
2	0	90
3	0.02	60
4	0.04	60
5	0.06	60
6	0.08	60
7	0.1	210
8	0.2	210
9	0.3	210
10	0.4	210
11	0.5	210
12	0.6	210
13	0.7	210
14	0.8	210
15	0.9	210
16	Y	210
17	0.9	210
18	0.8	210
19	0.7	210
20	0.6	210
21	0.5	210
22	0.4	210
23	0.3	210
24	0.2	210
25	0.1	210
26	0.08	60
27	0.06	60
28	0.04	60
29	0.02	60
30	0	60

Obtaining the polarization curves for the different configurations followed the JRC protocol [2]. The first stage of each test consisted of preconditioning the fuel cell under the operating conditions previously specified and introduced into the test bench configuration. Once the temperature, pressure and relative humidity conditions were reached, the load was turned on and the current density was increased. The current density was increased in steps of 0.1 A/cm^2 until a voltage of 0.5 V was reached. This value was noted because it was one of the values to be introduced in the table of conditions that automated the operation of the test bench in these experiments. The value of the current density was then increased until the maximum was found, which was set at value of 0.35 – 0.4 V to avoid degradation of the cell during the tests due to low voltages. This maximum was another of the values to be entered in the automation table.

Once these values were noted, it was possible to design the table shown in Table 3. First, the current density was kept constant at a value where the voltage was 0.5 V (X value in Table 3) for 3600 s to achieve stabilization of the conditions. Next, the cell was placed at 0 A/cm^2 or OCV conditions for a period of 90 s. Then there were increments of 0.02 A/cm^2 for 60 s until the current density reached 0.1 A/cm^2, and thereafter steps or increments of 0.1 A/cm^2 with a period of 210 s each. These increments reached the value shown as maximum and set as Y in Table 3. The next part of the table followed this process but in reverse, starting from the maximum value until the OCV was reached. Table 3 was repeated three times in the experiment to ensure greater reproducibility of the results and greater reliability of the data obtained. The test bench was programmed to acquire and save the data every 1 s of the test.

For post-processing of the data, the last 30 current density values were averaged and the current density and voltage values were plotted to obtain the polarization curves, as can be seen in the full paper [1].

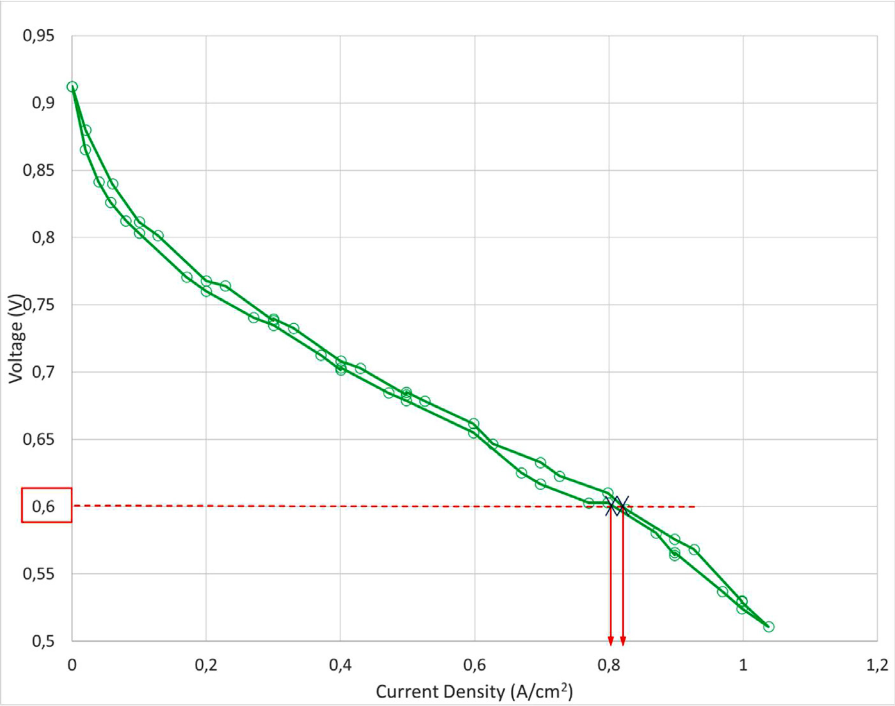

Fig. 14. Polarization curve to obtain the current density of FC-DLC test.

These graphs with the polarization curves were used to obtain the current density data required for the dynamic load cycling tests. The 100 % current density value used in the FC-DLC was defined as the average current density of the upward and downward polarization curve measurements to produce a voltage of 0.6 V. To do this, a straight line was drawn on the polarization curves at the 0.6 V value and its intersection with the double curve defined two current density values. The average of these two values was the current density value used in the FC-DLC test. Fig. 14 shows the process followed to obtain the current density value.

Once the 100 % current density value was defined, a table was created to automate the test bench conditions. Table 4 shows the points created for the dynamic load cycle test. First, a current density equal to that obtained at a voltage of 0.5 V (*X* value) was maintained for 3600 s to stabilize the operating conditions in the fuel cell. Then, a percentage of the current density was applied with respect to that defined as 100 %. For example, in point 3, 12.5 % of the current density defined as maximum was applied. The load percentages and run times are defined in the JRC protocol [2].

As occurred in the polarization curve tests, Table 4 was repeated three times in the experiment. The test bench was also programmed to save data every 1 s of the test.

During the performance of the polarization curve and dynamic load cycle tests, the CDM sensor was active, saving current density distribution and temperature distribution data. The CDM sensor used CurrentVIEW software to control the operating variables. The CDM sensor was connected to the test bench via 6 USB ports provided by the manufacturer. In the graphical interface of the CurrentVIEW software (Fig. 15), two zones can be distinguished, the left zone where the boxes with the values measured by the sensor and the buttons to control the program are located, and the right zone where a warning about the USB connections appears. If these connections are correct, the boxes are green and if they are not, they are red, as in the example in Fig. 15.

Table 4
FC-DLC test set points.

Set point no.	Current density (% A/cm^2)	Time (s)
1	X	3600
2	0	15
3	12.5	13
4	5	33
5	26.7	35
6	5	47
7	41.7	20
8	29.2	25
9	5	22
10	12.5	13
11	5	33
12	26.7	35
13	5	47
14	41.4	20
15	29.2	25
16	5	22
17	12.5	13
18	5	33
19	26.7	35
20	5	47
21	41.7	20
22	29.2	25
23	5	22
24	12.5	13
25	5	33
26	26.7	35
27	5	47
28	41.7	20
29	29.2	25
30	5	68
31	58.3	58
32	41.7	82
33	58.3	85
34	83.3	50
35	100	44
36	0	21

The functions of each of the boxes and buttons on the graphical interface are defined in Table 5.

Fig. 16 shows the sensor measurements at one point during the polarization curve test. As mentioned above, the negative sign of the current density values is highlighted.

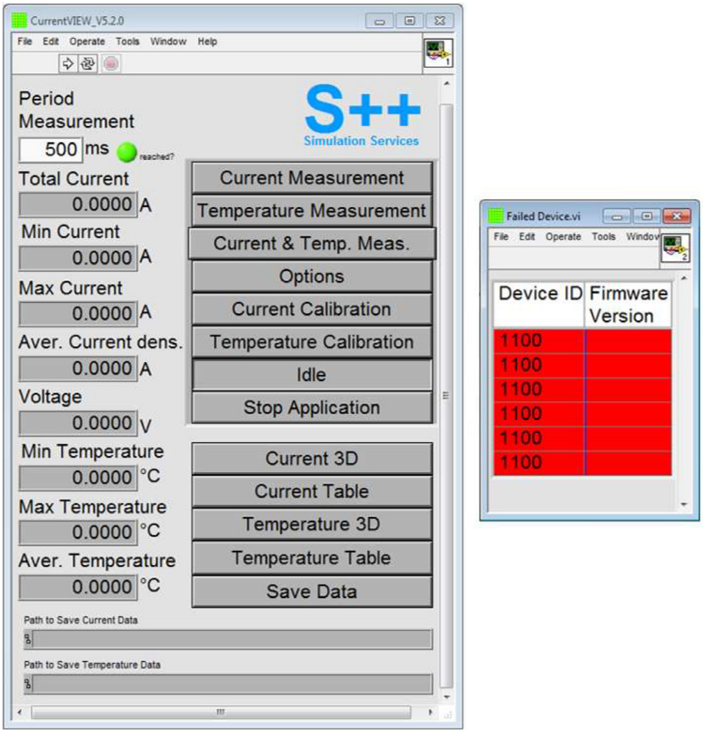

Fig. 15. Graphical interface of CurrentVIEW software.

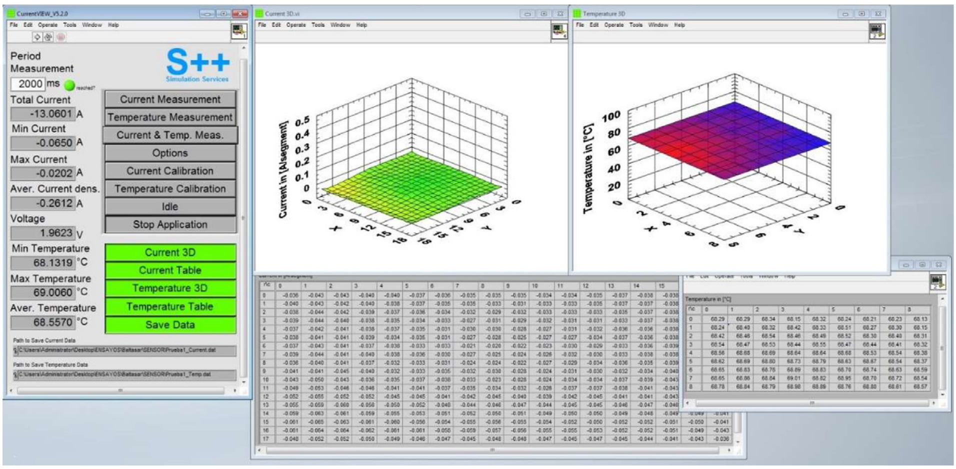

Fig. 16. Example of the CurrentVIEW software during the polarization curve test.

Table 5
Description of data and buttons of CurrentVIEW software.

Variable	Description	Unit
Current Measurement	When it is checked, CDM measures current density.	–
Temperature Measurement	When it is checked, CDM measures temperature.	–
Current & Temp. Meas.	When it is checked, CDM measures current density and temperature.	–
Options	Pressing this button opens a window where it is possible to modify the display of the graphs by changing the coordinate axes, scale colors, etc.	–
Current Calibration	Pressing it opens a window where the user can attach a .txt file of current densities provided by the manufacturer to calibrate the sensor.	–
Temperature Calibration	Pressing it opens a window where the user can attack a .txt file of temperatures provided by the manufacturer to calibrate the sensor.	–
Idle	This button is checked by default when the CDM sensor program is started.	–
Stop Application	When this button is pressed, the sensor stops taking measurements and the program returns to its initial state, with the setpoints showing a value of zero.	–
Current 3D	When pressed, it turns green and a window appears on the screen where the user can see the 3D graph of the current density distribution.	–
Current Table	When pressed, it changes to green color and the window appears on the screen where the user can see the table (18 × 18) with the current density measured by the sensor.	–
Temperature 3D	When pressed, it turns green and a window appears on the screen where the user can see the 3D graph of the temperature distribution.	–
Temperature Table	When pressed, it changes to green color and the window appears on the screen where the user can see the table (9 × 9) with the temperature measured by the sensor.	–
Save Data	Pressing it opens a window where the user has to indicate the destination directory for a .txt file that saves the temperature data and another .txt file that saves the current density data. Once the destination of these files has been indicated, the button turns green and the program begins to save the data measured by the sensor, with a saving period equal to the period defined as data acquisition in the set point (Period Measurement).	–
Period Measurement	Period in which the program measures or updates the data obtained with the CDM sensor.	ms
Total Current	Total current density measured by the sensor. Since the current densities are saved in 18 × 18 data arrays, this total value is the sum of all these values.	A
Min Current	Indicates the minimum current density obtained by the sensor, i.e., the minimum value of the 18 × 18 matrix of current densities.	A
Max Current	Indicates the maximum current density obtained by the sensor, i.e., the maximum value of the 18 × 18 matrix of current densities.	A
Aver. Current dens.	The graphical interface has an error in this set point because the unit would be A/cm^2 instead of A. Therefore, in this set point, the total current density is divided by the active area of the sensor, in this case 50 cm^2.	A $\downarrow$ A/cm^2
Voltage	Reference voltage.	V
Min Temperature	Indicates the minimum temperature obtained at the sensor, i.e., the minimum value of the 9 × 9 matrix of temperatures.	°C
Max Temperature	Indicates the maximum temperature obtained at the sensor, i.e., the maximum value of the 9 × 9 matrix of temperatures.	°C
Aver. Temperature	Indicates the average temperature of the fuel cell, which is the sum of all data in the temperature matrix divided by the total number of data (81).	°C

Limitations

Not applicable.

Ethics Statement

This work does not contain any studies with humans, animals from protected areas, endangered animals or any data collected from social media platforms. The authors declare that they have followed the general ethics rules for scientific research and publishing.

Data Availability

PEMFC_Parallel-Serpentine (Original data) (idUS)

CRediT Author Statement

Baltasar Toharias: Conceptualization, Data curation, Formal analysis, Investigation, Methodology, Software, Validation, Visualization, Writing – original draft, Writing – review & editing; **Christian Suárez:** Conceptualization, Data curation, Formal analysis, Investigation, Methodology, Software, Validation, Visualization, Writing – review & editing; **Alfredo Iranzo:** Conceptualization, Investigation, Methodology, Supervision, Validation, Writing – review & editing; **María Salva:** Data curation, Investigation; **Felipe Rosa:** Funding acquisition, Project administration, Resources.

Acknowledgements

This work has been funded through Grant TED2021-130706B-I00 financed via MICIU/AEI/10.13039/501100011033 and the European Union NextGenerationEU/PRTR.

Declaration of Competing Interest

The authors declare that they have no known competing financial interests or personal relationships that could have appeared to influence the work reported in this paper.

Supplementary Materials

Supplementary material associated with this article can be found, in the online version, at doi:10.1016/j.dib.2024.110392.

References

[1] C. Suárez, B. Toharias, M. Salva, A. Chesalkin, F. Rosa, A. Iranzo, Experimental dynamic load cycling and current density measurements of different inlet/outlet configurations of a parallel-serpentine PEMFC, Energy 283 (2023) 128455, doi:10.1016/j.energy.2023.128455.
[2] G. Tsotridis, A. Pilenga, G. De Marco, T. Malkow, EU harmonised test protocols for PEMFC MEA testing in single cell configuration for automotive applications, JRC Sci. Policy Rep. 27632 (2015) 21–23.
[3] S. Zhou, L. Rasha, L. Xu, W. Du, P. Shearing, M. Coppens, D. Brett, R. Jervis, Nonuniform compensation of current density distribution in polymer electrolyte fuel cells by local heating, Energy Convers. Manag. 297 (2023) 117717, doi:10.1016/j.enconman.2023.117717.
[4] W. Gao, X. Zhang, F. Gong, Z. Liu, Z. Zhang, C. Wang, Water flooding diagnosis of proton exchange membrane fuel cell based on current density scanning, J. Electroanal. Chem. 952 (2024) 117929, doi:10.1016/j.jelechem.2023.117929.
[5] F. Ding, T. Zou, T. Wei, L. Chen, X. Qin, Z. Shao, J. Yang, The pinhole effect on proton exchange membrane fuel cell (PEMFC) current density distribution and temperature distribution, Appl. Energy 342 (2023) 121136, doi:10.1016/j.apenergy.2023.121136.
[6] S++ Simulation Services, 2023 http://www.splusplus.com/measurement/en/csshunt.html (Accessed 29 November 2023).